

GIS and Remote Sensing Assessment of Landslide Susceptibility along the Cameroon Volcanic Line: West Region, Cameroon

Raphel Etoyiva Abine (✉ raphel.abine@myport.ac.uk)


University of Portsmouth School of Environment, Geography and Geosciences <https://orcid.org/0000-0002-5287-9390>

Research Article

Keywords: Cameroon, GIS, Landslide susceptibility, Multi-criteria decision Analysis, Cameroon Volcanic Line, Remote sensing

Posted Date: August 20th, 2021

DOI: <https://doi.org/10.21203/rs.3.rs-819468/v1>

License:  This work is licensed under a Creative Commons Attribution 4.0 International License.
[Read Full License](#)

Abstract

The physical and tectonic setting exposes the western part of Cameroon to natural and anthropogenic hazards. Small scale landslides with devastating effects are recurrent along the Cameroon Volcanic Line. Limited studies have addressed the susceptibility to sliding in the area. This study therefore aimed at producing a landslide susceptibility map of the West Region to aid local and national authorities in land use planning and policy to minimise loss. Eleven conditioning and triggering factors were selected to investigate landslide susceptibility in the study area. These factors include; slope angle, lithology, soil, slope aspect, elevation, rainfall, geological faults, land use, normalised difference vegetation index, roads and river networks. These factors were assigned weights using the analytical hierarchy process. The weighted linear combination technique was used to derive landslide susceptibility indices and the susceptibility map. The map was reclassified into five classes; very low, low, moderate, high and very susceptibility class. About 16% (2180 km²) of the study area lies within the high to very high class while 47% (6512 km²) is found within the moderate class. Steep slopes, weathered volcanic rocks and thick soil cover at high elevations control the distribution of landslides while high intensity rainfall is the main triggering factor. Residential houses and road infrastructures along steep slopes are the most vulnerable to sliding. Site specific assessment needs to be conducted in order to implement effective mitigation measures.

1. Introduction

On annual basis, over 1000 lives and property damage worth over \$4 billion are lost as a result of landslides (EM-DAT 2007). Of all the natural hazards in 2019, about 11% (44) were landslides leading to over 1,293 deaths (EM-DAT 2019). Studies show that most lives lost as well as property damage could be prevented if sufficient information and preventive measures were in place before a landslide event (Rajakumar et al. 2007; Pardeshi et al. 2013; Kavzoglu et al. 2014). In many developing countries like Cameroon (Fig. 1b), several challenges are faced ranging from basic needs such as food, shelter, water and sanitation, health care, quality education, increase population growth, the prevalence of diseases, conflicts and climate change (Aka et al. 2017; Kganyago and Mhangara 2019). As a result of an increase in urban population and inadequate infrastructures, more unplanned development is taking place in unstable terrains increasing the likelihood of susceptibility to slides (Moeyersons et al. 2004). For better land use, urban planning and mitigation of the impact of landslides, it is imperative to understand the causes, spatial distribution and to map areas liable to future landslides (Che et al. 2012; Vojtekova and Vojtek 2020).

The advancement in geospatial technology such as global positioning system (GPS), geographic information system (GIS) and remote sensing has contributed to hazard assessment, risk identification and disaster management (Akbar and Ha 2011). GPS is a satellite-based navigation system that provides geolocation information and time anywhere in the world (Gili et al. 2000; Coe et al. 2003). Several studies have demonstrated the use of GPS technologies in mapping landslides (Gili et al. 2000; Malet et al. 2002; Coe et al. 2003; Wang et al. 2012; Calcaterra et al. 2012; Cina and Piras 2015). GIS technology is

designed to collect, store, process, analyse, manage and present geographic or spatial data. It has been widely applied in the study of landslides in recent decades (Van Westen 2000; Van Westen et al. 2003; Shahabi and Hashim 2015; Al-Umar et al. 2020). Remote sensing is the science and art of acquiring information about an object on the earth's surface without being in physical contact with it. Remote sensing has been applied in several studies for landslide hazard zonation (Lui and Wu 2016; Francioni et al. 2019; Shi et al. 2020; Zhong et al. 2020).

Different methods and techniques have been employed in determining landslide susceptibility zones these include; deterministic, heuristic, statistical and multi-criteria decision analysis (Guzzetti et al. 1999; Dai & Lee 2002; Donati & Turrini 2002; Santacana et al. 2003; Durman et al. 2005; Ruff and Czurda 2008; Ahmed 2015; Ali et al. 2019, Vojtekova and Vojtek 2020). They can be grouped under two broad heading; qualitative and quantitative methods. Qualitative methods are subjective and present the landslide susceptibility maps in descriptive terms whereas quantitative methods give rise to numerical estimation in terms of the probability of occurrence of a landslide in a given zone (Park et al. 2013). The heuristic method relies on the investigator's knowledge of past landslide occurrences, causes and factors that contribute to slope instability. It is, therefore, a qualitative method that involves the ranking and weighting of causative factors according to their importance in contributing to slope failure (Leoni et al. 2015; Stanley and Kirschbaum 2017; Huang et al. 2020). A statistical method is a quantitative approach which deals with the analysis of the relationship between causative factors and prior landslide distribution. Statistical techniques commonly used in landslide hazard mapping include bivariate, multivariate, logistic regression and artificial neural networks (Dhakal et al. 2000; Yalcin et al. 2011; Pradhan 2013; Fernandez et al. 2013; Anbalagan et al. 2015; Reichenbach et al. 2018; Mergili et al. 2019). Deterministic models are based on the analysis of existing slope failure mechanisms through physical models calibrated using onsite and laboratory tests (Park et al. 2013; Cuirlo et al. 2017).

Several factors are taken into consideration in landslide susceptibility mapping. Determining the contribution of each parameter to landslide susceptibility mapping is a complex problem. The analytical hierarchy process (AHP) is a multi-criteria technique for landslide hazard mapping that makes use of pairwise comparison of causative factors and expert knowledge of the investigator in assigning weights or priority scale to the factors (Saaty 2008; Park et al. 2013; Feizizadeh and Blaschke 2013; Feizizadeh et al. 2014; Arca et al. 2018). The AHP method operates under four facets; formulation of the problem, determination of intended goal and alternatives, construction of pairwise comparison matrix, determining factor weights and deriving landslide susceptibility index using an aggregation method. Park et al. (2013) investigated landslide susceptibility in Inje area in Korea using frequency ratio, AHP, logistic regression and artificial neural network and revealed that AHP performed well compared to the other methods. A similar outcome was obtained by Kavzoglu et al. (2014) in Trabzon Province in Turkey where multicriteria decision analysis (MCDA) outperformed logistic regression in determining landslide susceptibility zones. Vojtekova and Vojtek (2020) used the MCDA technique in mapping landslides in Slovakia, they obtained a satisfactory result.

The physical and tectonic setting of Cameroon coupled with changing climatic conditions exposes the western part of the country to both natural and anthropogenic hazards (Ayonghe et al. 1999, 2002, 2004; Ayonghe and Ntasin 2008; Buh et al. 2009; Che et al. 2011, 2012; Diko et al. 2012; Guedjo et al. 2013; Wotchoko et al. 2016). Several natural and anthropogenic hazards have been recorded in Cameroon including; flooding, volcanic eruption, earthquakes, landslides and volcanic gas emission (Ayonghe and Ntasin 2008; Buh et al. 2009; Kometa 2012; Wantim et al. 2013). The western part of Cameroon has been hit by small but recurrent landslides leading to over 146 deaths, thousands of persons displaced and millions of dollars in property loss in the past three decades (Ayonghe et al. 2004; Zogning et al. 2007; Ngole et al. 2007; Thierry et al. 2008; Che et al. 2011; Wotchoko et al. 2016; Ntchantcho et al. 2017). Most studies of landslides in this region have focused on mapping their occurrences and distribution as well as damages caused (Ayonghe et al. 1999, 2004; Che et al. 2011; Tchindjang, 2013). While Che et al. (2012) produced a landslide susceptibility map for Limbe (a section of the tectonically active Cameroon Volcanic Line), the recent landslide in Gouache neighbourhood in Bafoussam (Fig. 1c), an area with no historical landslide record sheds light on the necessity to map the entire region. This study is therefore aimed at producing a landslide hazard zonation map that will be used by local and national authorities for land use planning and policy to minimize loss. The objectives of this work are; to identify areas more likely to be affected by landslides in the future using satellite images and the analytical hierarchy process, to understand the factors leading to slope instability in the region from the multicriteria decision analysis, to identify settlements and land uses in the high-risk zone for possible relocation or preventive measures, to increase awareness and add to the already growing data on hazards in Cameroon.

2. Study Area

The study area is situated in the geopolitical West Region of Cameroon within longitude 10° 30' 00" and latitude 5° 30' 00" (Fig. 1c). It is the smallest of the ten regions of Cameroon with a surface area of approximately 13892 km², a total population of 1,921,590 as of 2015 and a high population density of 140/km² (Tesi, 2018). Bafoussam, the political capital of the West Region is located about 336 km from the national capital, Yaounde. The area has a moderate Equatorial climate resulting from high elevation and high humidity. Temperatures vary between 15°C to 28°C. This region experiences high rainfall averaging 1000–2000 mm/year (Tesi, 2018).

The topography of the West Region is generally mountainous with elevations ranging from 224 to 2744 metres above sea level. As a result of the mountainous terrain, fast-flowing rivers are ubiquitous. Several crater lakes have developed from collapsed volcanoes. The area has a variable soil type comprising of ferrallitic soils and alluvial soils derived from the weathering of plutonic and volcanic rocks.

The original forest vegetation has been cleared for agriculture giving rise to grassland vegetation. Patches of Woodland Savannah of the Sahel type are found distributed within the area. Plantation farming is practised on a small scale, with coffee, cocoa, tea and tobacco as the main cash crops. Livestock farming includes; cattle, sheep and goat rearing. Poultry and piggery farming is also

increasingly practised in recent years. The region is well known for artistic and craftsmanship which involves the production of high-quality ceramics from clay, woodworks, brass and bronze casting and cotton textiles (Tesi, 2018).. It is the most accessible region in Cameroon comprising of several paved roads linking Yaounde, Douala and Bamenda.

The geology of Cameroon is comprised of Precambrian basement rocks, sedimentary rocks of Cretaceous Period and Cenozoic Era and volcanic rocks of Cenozoic Era (Toteu et al. 2001; Assah et al. 2014). The Precambrian basement is subdivided into the Congo Craton (Archaean and Paleoproterozoic terranes) and the Central African Fold Belt (CAFB). The CAFB is a Neoproterozoic Orogen associated with Trans-Saharan Belt of West Africa which is linked to the Brasiliano Orogen of NE Brazil (Van Schmus et al. 2008). Three tectonic units have been identified in this belt; North Cameroon Domain, Central Cameroon Domain and South Cameroon Domain. The study area lies within the central domain comprised of intrusions of Pan-African granitoids emplaced through the control of zones of weaknesses along the Cameroon Volcanic Line (Kouankap Nono et al. 2013). The Cameroon volcanic line (CVL) is a chain of oceanic and continental volcanoes extending from the Pagalu Island to Lake Chad. It is oriented NE-SW extending over a length of 1600 km and a width of ~ 100 km (Marzoli et al. 2000; Suh et al. 2003). The geology of the study area is made up of three main units; 1) garnet-bearing gneiss, migmatites and amphibolite 2) Granitoids 3) basaltic rocks comprised of basaltic lava and dolerite dykes (Kouankap Nono et al. 2010; 2013).

3. Data And Methods

3.1 Data Sources for Landslide Conditioning Factors

Various factors have been selected to investigate landslide susceptibility in the study area. Table 1 details the type and source of data used in the assessment of landslides susceptibility. Thematic maps were generated from these data in a GIS environment. Given the paucity of literature in the study area, the selection of factors was based on a review of literature that conducted comparable assessments of landslide susceptibility in areas with similar characteristics (Ayonghe et al. 1999; Ayonghe and Ntasin 2008; Ntasin et al. 2009; Ngatcha et al. 2011; Che et al. 2011, 2012).

Landsat 8 operational land imager (OLI) images were downloaded from the United States Geological Survey website (Table 1). These images were layer stacked in ERDAS Imagine 2018 employing contrast enhancement and feathering techniques (Kumar 2005).

3.2 Multicriteria Decision Analysis

Multicriteria decision analysis (MCDA) is a GIS-based method for decision making through the integration of geographic data and subjective judgements (Malczewski 1999).

3.2.1 Analytical Hierarchy Process

An analytic hierarchy process (AHP) is a form of MCDA quantitative method for decision making using factor weights through pairwise comparison (Saaty 1987). This method measures both tangible and intangible variables through relative weights given to each variable based on the preference of the researcher. It has been widely applied in MCDA, planning, natural and man-made resource allocation, and conflict resolution (Saaty 1986; Kamar and Anbalagan 2016; Jazouli et al. 2019; Nzotcha et al. 2019; Vargas and Zoffer 2019).

The AHP method has three distinct facets; decomposition, comparative judgment and synthesis of priorities. A complex problem is broken down into a hierarchy of variables or factors using a pairwise comparison matrix, factors are assigned weights on a nine-point scale see Table 2 (Eastman 2012). The factors are arranged in a matrix form with the same number of rows and columns with scores assigned to each factor in comparison to other factors (Saaty 1977). The scale of comparison of paired factors was determined from a careful literature review of landslide occurrences along the Cameroon Volcanic Line (Buh 2009; Diko 2012; Diko et al. 2012; Guedgjeo et al. 2013; Wotchoko et al. 2016; Ntchantcho et al. 2017). After generating the pairwise comparison matrix, weights of each factor were determined by calculating the principal Eigenvector of a square reciprocal of the metrics making sure they sum up to unity (Malczewski 1999; Ahmed 2015). The pairwise comparison is based on two intrinsic questions to determine criterion or factor more important than the others and the extent based on a ratio scale of 1/9 to 9 (Table 2). The AHP calculation was undertaken using Microsoft excel.

To validate the results of the pairwise comparison metrics and factor weights, the consistency index (CI) and the consistency ratio (CR) was determined (Eastman 2012). The consistency index is given by

$$CI = \frac{\lambda_{max} - n}{n - 1} \dots\dots\dots (1)$$

Where CI = consistency index

λ_{max} = normalized highest Eigenvalue of the pairwise matrix

n = number of factors (11 factors in this study)

The consistency ratio shows how random the matrix ratings were selected as given by Saaty (1980).

$$CR = \frac{CI}{RI} \dots\dots\dots (2)$$

Where CR = consistency ratio

RI = Random Index

Random index (RI) has been proposed by Saaty (1987) and presented in Table 3

A consistency ratio of 0 implies perfect ratings of factors, CR of > 0.1 implies inconsistency of the ratings. Saaty (1980) suggested a re-evaluation of factor ratings for CR > 0.1.

The result of a pairwise comparison matrix gives rise to factor weight which is then aggregated to generate a landslide susceptibility map (Gorsevski et al. 2006; Jian & Eastman 2000; Boroumandi et al. 2015). Several methods have been employed to aggregate factor weights in generating susceptibility maps. These include; weighted linear combination, weighted sum, weighted overlay and ordered weighted average (Eastman and Jain 1995; Jain and Eastman 2000; Malczeswki 2004; Ahmed 2015; Vojtekova and Vojtek 2020).

3.3 Data Preparation

3.3.1 Landslide Inventory

The first step involved in producing a landslide susceptibility map is to generate an inventory of past landslides (Abedini and Tulabi 2018). Following the law of uniformitarianism, landslides are likely to occur in areas where past slope failures have been recorded (Guillard and Zezere 2012; Ge et al. 2018). Landslide inventory map can be used as a means for assigning weights to landslide triggering factors (Kumar et al. 2018). These maps can be generated from aerial photographs, field surveys, satellite images and existing landslides. Fourteen landslides were determined in the study area from the review of literature (Table 4) and the classification of satellite images (Fig. 1c).

3.3.2 Land use and Normalized Difference Vegetation Index

Land use map was generated from the Landsat 8 OLI satellite image through supervised classification using maximum likelihood (Lu and Weng 2007). False-colour composite images and Google Earth were used to obtain training data through the polygon method. Five landcover classes were identified; water body, agricultural land, built-up area, vegetation and bare soil (Fig. 2a).

Due to the influence of vegetation coverage on slope stability, normalized difference vegetation index (NDVI) was carried out to characterize vegetation extent in the study area Eq. 4

$$NDVI = \frac{IR - R}{IR + R} \dots\dots\dots (4)$$

Where NDVI = normalized difference vegetation index

IR = Infrared (band 5)

R = Red (band 4)

NDVI analysis results in an output of values ranging from -1 to 1 where the negative values represent clouds, water and snow (Zaitunah et al. 2018). NDVI values of 0–0.1 represent barren land, rocks and soils while values of 0.6–1 represent dense vegetation (Fig. 2b).

3.3.3 Elevation

A 30m resolution shuttle radar topography mission (SRTM) digital elevation model (DEM) was downloaded from the USGS website. The average elevation of the study area is 155m, the lowest point is 224m and the highest point is 2744m (Fig. 2c). Generally, areas with higher elevations are more susceptible to landslides. The elevation generated was reclassified into five classes to determine the level of contribution of each category to landslides.

3.3.4 Slope

The digital elevation model (DEM) was used to generate a slope map, the slope in the study area ranges from 3.64° to 77.33° with an average of 40.49° (Fig. 2d). Areas with steep slopes are often more prone to landslides (Kavzoglu et al. 2014). The Slope was reclassified into five classes following the recommendation of Kumar et al. (2018). The categories are; flat to gentle, moderate, fairly moderate, steep and very steep slopes (Fig. 2d).

3.3.5 Aspect

Aspect refers to the orientation of a slope from 0° to 360° . Sunlight exposure, drying winds, rainfall and discontinuities are factors associated with slope aspect which influences the degree of susceptibility to landslides (Dai et al. 2001). Nine slope directions were generated and reclassified according to their contribution to landslide susceptibility (Fig. 2e).

3.3.6 Geology

A scanned geologic map of Cameroon was georeferenced, the geology of the study area was digitised into polygons that were converted to raster format. Four lithologies were identified; pre-syn tectonic granitoids, syn-post tectonic granitoids, orthogneiss, and volcanic rocks (Fig. 2f). The area has highly weathered volcanic rocks which have been identified in some studies as landslide-prone lithologies (Che et al. 2011).

3.3.7 Soils

The stability of slopes depends on the soils they contain (Sartohadi et al. 2018; Schiliro et al. 2019). The soil map was digitized from the African groundwater Atlas map. The soil atlas was converted from shapefile to a 30 m raster file in Arcmap. Five soil types of varying permeability and susceptibility to landslides were derived; andosols, loxisols, luvisols, stagnosols, and vertisols (Fig. 2g). Luvisols are the dominant soil type in the study area. Soils capable of holding water have a higher level of susceptibility (Nandi and Shakoor 2009).

3.3.8 Rainfall

The average monthly rainfall data of the study area from the year 2000 to 2020 were downloaded from the NASA Earth Data website, this data was interpolated to generate the rainfall map (Fig. 2h). The average monthly rainfall ranges from 97 to 171mm/month. The rainfall data were reclassified into five classes representing susceptibility levels.

3.3.9 Distance to Road and River

Road cut and drainage density have been shown to influence slope stability (Van Buskirk et al. 2005; Yalcin et al. 2011). Road and river network data was downloaded from the OpenStreetMap data repository as shapefiles. The shapefiles were converted to raster data with a resolution of 30m. The Euclidean distance function in ArcMap was used to derive the distance to roads and rivers. Five classes were generated for both distances to road and distance to rivers (Fig. 2i and j).

Construction of roads along steep slopes leads to slope instability which is exacerbated by vehicle movement and high-water retention capacity in cracks that result (Yalcin et al. 2011; Awahdeh et al. 2018).

3.3.10 Distance to Fault

From the georeferenced geologic map of Cameroon, faults were digitised into line features (Fig. 2k). The multiple ring buffer function was used to generate a distance to faults. Five classes were derived with intervals of 5km.

3.4 Aggregation of Factor weights

In this study, the weighted linear combination (WLC) method was used (Appendix). This method is customized in many GIS platforms and it is flexible in combining thematic maps of conditioning factors to generate landslide susceptibility maps (Feizizadeh and Blaschke 2013). It requires the standardization of classes within each factor to a common numeric scale. The factor classes are multiplied by the weights obtained from the comparison matrix and their results summed to obtain the landslide susceptibility index (Eq. 3).

$$LSI = \sum_{j=1}^n W_j X_{Zij} \dots \dots \dots (3)$$

Where LSI = Landslide Susceptibility Index

W_j = Weight value of causative factor j

Z_{ij} = Weight value of class i of causative factor j

The landslide susceptibility indices generated was reclassified to derive the landslide susceptibility map using the Jenk classification method. The map was reclassified into five classes; very high, high, moderate, low and very low susceptibilities (Fig. 3).

4. Results And Analysis

4.1 Landslide susceptibility Map

Landslide susceptibility map was generated through the weighted linear combination method using 11 landslide conditioning factors (Fig. 3, Table 5). The landslide susceptibility map was classified into five classes using the natural break (Jenk) method; very low, low, moderate, high and very high susceptibility. The Jenk method is a data clustering technique used to determine the best grouping of values into different classes by minimising the deviation of each class from the class mean while maximising the class deviation from the means of other groups (Raja et al. 2017).

To create a landslide susceptibility map using the AHP technique, a pairwise comparison matrix is constructed. The matrix is used in assigning factor ratings and for calculating factor weights (Tables 5 and 6). The consistency ratio determines the degree of consistency in assigning the factor weights. In this study, the consistency ratio (CR) is < 0.1 .

The area and percentage coverage of five landslide classes is presented in Table 7. From Table 7, the medium landslide category has the highest area coverage of 6512 km² (47%) followed by the low category 3149 km² (23%). The very low landslide category occupies 2051 km² (15%). The lowest area coverage is occupied by the high landslide category 230 km² (2%). The very high landslide category covers 1950 km² (14%) of the study area. Therefore, about 16% (2180 km²) of the study area falls within the high and very high landslide category (Table 7).

4.2 Landslide Model validation

To determine how successful the model is in predicting landslide susceptible zones, the landslide inventory was superimposed on the landslide susceptibility map see Table 7. From Table 7 43% of landslide inventory falls within the high to very high susceptibility class. About 36% of landslide falls within the medium class while 21% falls within the low susceptibility class. The result shows that no landslide has been recorded in the very low landslide susceptibility class.

5. Discussion

5.1 Selection and weighting of conditioning factors

The reliability of the landslide susceptibility map generated depends on the selection of appropriate conditioning factors, the objective weighting of factors and the suitability of the model used (Donati and Turrini 2002; Broeckx et al. 2018). The spatial scale of analysis has been identified as a determinant for

choosing conditioning factors. For local spatial scale (1–30 km²), it is recommended that more accurate input data be used (Zezere et al. 2017; Vojtekova and Vojte, 2020). At regional, national or global scale, it is usually difficult to use site-specific data due to the variability of terrain features over large scales, therefore, more generalised conditioning factors are adopted (Kirschbaum et al. 2010; Petley et al. 2002; Van Den Eeckhaut et al. 2006; Van Westen et al. 2008; Holec et al. 2013; Manzo et al. 2013; Broeckx et al. 2018). The selection of conditioning factors was based on the review of literature which revealed similar slope failures along the Cameroon volcanic line (Ayonghe et al. 2004; Ayonghe and Ntasin 2008; Che et al. 2011, 2012; Guedjeo et al. 2013).

A major challenge commonly encountered in landslide susceptibility analysis is the subjectivity involved in assigning weights to conditioning factors (Erener et al. 2016). To objectively assign weights to these factors, some authors have suggested the use of landslide frequency ratio and weight of evidence (Van Western et al. 2003; Regmi et al. 2010). Donati and Turrini (2002), superimposed thematic maps of conditioning factors on landslide inventory map to determine factors most relevant to landslide susceptibility in Valnerina, Italy. This approach was adopted in the study.

Several GIS techniques have been employed to assess landslide susceptibility. Kavzoglu et al. (2014) compared multi-criteria decision analysis (MCDA), support vector machine (SVM) and logistic regression (LR) to determine landslide susceptibility in northeast Turkey. It was found that MCDA using the analytical hierarchy process (AHP) technique was far superior to logistic regression. Furthermore, Ahmed (2015) examined three different MCDA methods in the Chittagong area in Bangladesh and obtained favourable results, though the weighted linear combination out-performed both AHP and ordered weighted average (OWA). In a similar study, Feizizadeh and Blaschke (2013) noted that the AHP method out-performed both WLC and OWA in a landslide study in the Urmia lake basin, Iran. As a result of the successes in the application of MCDA methods (Ayalew et al. 2004; Kumar and Anbalagan 2016; de Brito et al. 2017; Gigovic et al. 2019; Jazouli et al. 2019; Vojtekova and Vojtek 2020), coupled with its ability to integrate different data layers with varying uncertainties, the MCDA technique was chosen for this study. The result obtained is representative of the study area when compared to the landslide inventory.

5.2 Causes of sliding in the area

Several factors interplay in making an area liable to sliding, both natural and anthropogenic influences on slope stabilities can be distinguished. Steep slopes (35–77°) and high elevation (700–2700 m) are responsible for most of the sliding in the study area this is in accord with the results obtained from areas with similar characteristic (Awawdeh et al. 2018; Nicu 2018; Bera et al. 2019). Weathered volcanic rocks and thick soil cover on steep slopes also contribute to slope instability in the study. This result is similar to that reported by Che et al. (2012) and Buh (2009) in the Limbe Municipality. Earthquakes have been identified as a landslide triggering factor (Kefer 2002; Yin et al. 2009; Bai et al. 2012; Chen et al. 2012; Xu et al. 2012; Zhao et al. 2018; Osanai et al. 2019; Matossian et al. 2020). Seismic induced landslides have been reported along the Cameroon Volcanic Line (Ayonghe et al. 1999). Buh (2009) noted that earthquakes along the CVL are of low intensity and have no major association with landslides. An

indirect link may be associated with the development of tension cracks leading to high infiltration of water and eventual slope failure. This is the scenario in the study area as evidence from the strike slip faults cutting through the high-risk zones (Kouankap Nono et al. 2010, 2013). As the case may be with several tropical terrains, studies point to a high intensity rainfall (100mm/day) over a short duration as the main trigger of landslides in Cameroon (Buh 2009; Guedjeo et al. 2013; Wotchoko et al. 2016; Ntchantcho et al. 2017).

Rivers and roads appear to have less influence on landslide susceptibility in the study area. This is in contrast to the result of Che et al. (2012) in Limbe where road cuts and slope erosion by rivers contributed to landslides. This could be explained by the fact that considerable preventive measures; retaining walls and slope terrace have been constructed along major high ways. Land use change is one of the anthropogenic factors leading to slope failure (Chen and Huang 2013; Reichenbach et al. 2014). This is confirmed by the work of Alcantara-Ayala et al. (2006) in Sierra Norte, Mexico where 72% of landslides occurred in areas with low vegetation cover resulting from deforestation. As a result of population growth and the construction of buildings along steep slopes with no engineering considerations, land use change will continue to have an impact on landslide susceptibility in the study area.

5.3 Uncertainties in landslide model assessment

In the MCDA using the AHP technique, errors may result from assigning incorrect factor weights. For example, Ahmed (2015) noted that high susceptibility class was found at low elevation which is not normally associated with landslides. This resulted from the assignment of weight to some factors which occurred both in high as well as low elevations. Therefore, results obtained using MCDA may have inherent errors. As a result of the subjectivity in assigning factor weights, an incorrect weight assignment affects the accuracy of the susceptibility map generated (Kritikos and Davies 2011). Another source of error is the incorrect pairwise comparison of factors. Ahmed (2015) suggested that different combination of factors be taken into consideration in order to derive the most appropriate factor weights. To ensure appropriate rating and weighting of factors, Saaty (1980) and Eastman (2012) developed the consistency index and consistency ratio for determining the randomness in assigning factor weights which in turn affects the quality of the susceptibility map generated. The consistency ratio for both factors and sub-factors is less than 0.1 (Tables 5 and 6) which is the cut-off set by Saaty (1980) for revising factor weighting. Therefore, the susceptibility map created in this study is of good quality.

The quality of the data set used may also introduce errors in the map generated. The spatial resolution of satellite images and SRTM DEM constraints its effectiveness in studying landslides which also affects the thematic maps derived (Shahabi et al. 2012; Shahabi and Hashim 2015; Ji et al. 2020). Petley et al. (2002) were successful in identifying just 25% of landslides in Nepal's highlands using Landsat 7 ETM + images with a 30 m spatial resolution pansharpened to 15 m. Nichol and Wong (2005) showed that at a 1m spatial resolution, satellite images may not be suitable for identifying small scale landslides (< 10 m wide). Therefore, a 30m spatial resolution satellite image and DEM is not suitable for this study given

that most of the landslides along the CVL are of small scale (Zogning et al. 2007; Thierry et al. 2008; Zangmo et al. 2009; Wotchoko et al. 2016). However, this is the data set freely available for the study.

When georeferencing and digitising raster data, errors are usually introduced (Pearson 2006). To reduce the error margins, ground control points were carefully selected and a first order polynomial was used to georeference the geologic, faults and soil maps. Topological rules (no overlapping, no dangle lines and no pseudo lines) were used to ensure accurate digitising of faults, geology and soil maps (Pearson 2006). The rainfall data obtained from the NASA Earth Data website was interpolated using the kriging technique (Ly et al. 2013). An averaging algorithm was used to fill in the missing time gap data (Acker and Leptoukh 2007). Data acquired from Open Street Map (OSM) may be inaccurate resulting from the contribution of data from volunteers with little to no geospatial knowledge. However, the availability of high-resolution aerial and satellite images enables efficient data collection and validation of digitised features (OSM 2020).

5.4 Risk Assessment

The ultimate aim for undertaking a landslide susceptibility assessment is to determine land-use types that might be affected in an event of a landslide in order to implement mitigation measures (Varness 1984; Awawdeh et al. 2018). A qualitative approach was used to determine the risk associated with landslide categories in agricultural land, urban area and road infrastructures. Some roads in the study area are found within high-risk zone, for example, about 42 km of the Bafoussam-Foumban highway lies within the very high susceptibility class while 22 km passes along the high susceptibility class (Fig. 4). Similarly, the national road (N4) running from Douala-Bafoussam cuts across the moderate susceptibility class for over 58 km and the high category for about 6 km (Fig. 4). Furthermore, the Mbouda-Bamenda highway passes through the moderate susceptibility class for over 48 km.

Results show that about 10% of the urban area comprising of parts of Foumban, Foubot, Bafoussam, Santchou, and Mbouda falls within the very high class (Fig. 4). About 7% of the urban area including parts of Bafoussam, Bangante, Santchou lies within the high category. Over 30% of the urban area is located in the moderate susceptibility class. Residential houses built along unstable slopes have been identified as the most vulnerable to sliding. Another important land use which might be affected by landslides is agricultural land. Over 50% of agricultural land is found within the moderate susceptibility category. This has been identified in some studies as a landslide inducing factor as it involves the cutting down of trees and tilling of soils (Jazouli et al. 2019). A small portion of the agricultural land (4%) is found within the high to very high susceptibility class.

6. Conclusion

Several small but destructive landslides have hit the western part of Cameroon along the Cameroon Volcanic Line in the past three decades. With increase in urbanisation and construction of houses on steep slopes without engineering considerations landslides in the West Region of Cameroon are inevitable. This is exacerbated by changing climatic conditions leading to increase in rainfall regime. This

study therefore aimed at undertaking a landslide susceptibility assessment to aid local and national authorities in land use and policy planning to minimise the destructive effects of landslides. Eleven landslide conditioning factors were selected to investigate slope stability in the study area. Steep slopes, high elevations, weathered volcanic rocks and thick soil cover along steep slopes are identified as the major landslide causative factors. High intensity rainfall (110 mm/day) for over a period of 2–4 days is the main landslide triggering factor in the area. The landslide susceptibility map generated from the multicriteria decision analysis was subdivided into five classes; very low, low, moderate, high and very high susceptibility class. Roads and residential houses built along steep slopes are the most vulnerable infrastructures to slides. Agricultural land is less vulnerable to sliding as over 50% is found within the moderate susceptibility class. To curb the effect of landslides, some mitigation mechanism such as; tree planting, slope terracing, draining pipes, construction of retaining walls is proposed. In order to implement appropriate mitigation measures, it is recommended that site specific assessments be conducted to identify triggering factors in high to very susceptibility zones.

7. Declarations

Funding

No funding was received to assist with the preparation of this manuscript.

Conflict of interest

The author declares no conflict of interest

Availability of data

Code availability 'Not applicable'

Author's contribution

This work is an output from the author's MSc dissertation. It was conceived and produced by the author.

Acknowledgements

Raphel Etoyiva Abine is a Commonwealth Scholar funded by the UK government.

Harold Lovell is gratefully acknowledged for critiquing and improving the manuscript

8. References

1. Abedini M, Tulabi S (2018) Assessing LNRF, FR, and AHP models in landslide susceptibility mapping index: a comparative study of Nojian watershed in Lorestan province, Iran. *Environmental Earth Sciences* 77(11): 1–13. <https://doi.org/10.1007/s12665-018-7524-1>

2. Acker J G, Leptoukh G (2007) Online Analysis Enhances Use of NASA Earth Science Data. *Eos, Trans. AGU* 88, (2): 14 - 17.
3. Ahmed B (2015) Landslide susceptibility mapping using multi-criteria evaluation techniques in Chittagong Metropolitan Area, Bangladesh. *Landslides* 12(6): 1077–1095.
<https://doi.org/10.1007/s10346-014-0521-x>
4. Aka F T, Buh G W, Fantong W Y, Issa, Zouh I T, Djomou S L B, Ghogomu R T, Gibson T, Marmol del M A, Sigha L N, Ohba T, Kusakabe M, Yoshida Y, Tanyileke G, Nnange J M, Hell J V (2017) Disaster prevention, disaster preparedness and local community resilience within the context of disaster risk management in Cameroon. *Natural Hazards* 86(1): 57–88. <https://doi.org/10.1007/s11069-016-2674-5>
5. Akbar T A, Ha S R (2011) Landslide hazard zoning along Himalayan Kaghan Valley of Pakistan-by integration of GPS, GIS, and remote sensing technology. *Landslides* 8 (4): 527–540.
<https://doi.org/10.1007/s10346-011-0260-1>
6. Al-Umar M, Fall M, Daneshfar B (2020) GIS-based modeling of snowmelt-induced landslide susceptibility of sensitive marine clays. *Geoenvironmental Disasters* 7(1)
<https://doi.org/10.1186/s40677-020-0142-8>
7. Alcántara-Ayala I, Esteban-Chávez O, Parrot J (2006) Landsliding related to land-cover change: A diachronic analysis of hillslope instability distribution in the Sierra Norte, Puebla, Mexico. *Catena* 65(2): 152–165. <https://doi.org/10.1016/j.catena.2005.11.006>
8. Ali S, Biermanns P, Haider R, Reicherter K (2019) Landslide susceptibility mapping by using a geographic information system (GIS) along the China-Pakistan Economic Corridor (Karakoram Highway), Pakistan. *Natural Hazards and Earth System Sciences* 19(5): 999–1022.
<https://doi.org/10.5194/nhess-19-999-2019>
9. Anbalagan R, Kumar R, Lakshmanan K, Parida S, Neethu S (2015) Landslide hazard zonation mapping using frequency ratio and fuzzy logic approach, a case study of Lachung Valley, Sikkim. *Geoenvironmental Disasters* 2(1) <https://doi.org/10.1186/s40677-014-0009-y>
10. Arca D, Kutoğlu H, Becek K (2018) Landslide susceptibility mapping in an area of underground mining using the multicriteria decision analysis method. *Environmental Monitoring and Assessment* 190(12): <https://doi.org/10.1007/s10661-018-7085-5>
11. Asaah A V, Zoheir B, Lehmann B, Frei D, Burgess R, Suh C E (2015) Geochemistry and geochronology of the ~620 Ma gold-associated Batouri granitoids, Cameroon. *International Geology Review* 57(11–12): 1485–1509. <https://doi.org/10.1080/00206814.2014.951003>
12. Awawdeh M M, ElMughrabi M A, Atallah M Y (2018) Landslide susceptibility mapping using GIS and weighted overlay method: a case study from North Jordan. *Environmental Earth Sciences* 77(21): 1–15. <https://doi.org/10.1007/s12665-018-7910-8>
13. Ayalew L, Yamagishi H, Ugawa N (2004) Landslide susceptibility mapping using GIS-based weighted linear combination, the case in Tsugawa area of Agano River, Niigata Prefecture, Japan. *Landslides* 1(1): 73–81. <https://doi.org/10.1007/s10346-003-0006-9>

14. Ayonghe S N, Mafany G T, Ntasin E, Samalang P (1999) Seismically activated swarm of landslides, tension cracks, and a rockfall after heavy rainfall in Bafaka, Cameroon. *Natural Hazards*19(1): 13–27. <https://doi.org/10.1023/A:1008041205256>
15. Ayonghe S N, Ntasin E B, Samalang P, Suh C E (2004) The June 27, 2001 landslide on volcanic cones in Limbe, Mount Cameroon, West Africa. *Journal of African Earth Sciences*39(3–5):435–439. <https://doi.org/10.1016/j.jafrearsci.2004.07.022>
16. Ayonghe S N, Ntasin EB (2008) The geological control and triggering mechanisms of landslides of 20th July 2003 within the Bamboutos Caldera, Cameroon. *Journal of the Cameroon Academy of sciences* 7 (3): 191-204
17. Bai S, Wang J, Zhang Z, Cheng C (2012) Combined landslide susceptibility mapping after Wenchuan earthquake at the Zhouqu segment in the Bailongjiang Basin, China. *Catena*99: 18–25. <https://doi.org/10.1016/j.catena.2012.06.012>
18. Bera A, Mukhopadhyay B P, Das D (2019) Landslide hazard zonation mapping using multi-criteria analysis with the help of GIS techniques: a case study from Eastern Himalayas, Namchi, South Sikkim. *Natural Hazards*96(2): 935–959. <https://doi.org/10.1007/s11069-019-03580-w>
19. Bobrowsky P, Couture R (2014) *Landslide terminology, canadian technical guidelines and best practices related to landslides: a national initiative for loss reduction*. <https://doi.org/10.4095/293940>
20. Boroumandi M, Khamsehchiyan M, Nikoudel R N (2015) Using of Analytical Hierarchy Process for landslide hazard zonation in Zanjan Province, Iran. *Engineering Geology for Society and Territory* 2: 951-955. https://DOI: 10.1007/978-3-319-09057-3_165
21. Broeckx J, Vanmaercke M, Duchateau R., Poesen J (2018) A data-based landslide susceptibility map of Africa. *Earth-Science Reviews*, 185: 102–121. <https://doi.org/10.1016/j.earscirev.2018.05.002>
22. Buh G W (2009) Geographic information systems based demarcation of risk zones: the case of the Limbe Sub-Division – Cameroon. *Jàmbá: Journal of Disaster Risk Studies*2(1): 54–70. <https://doi.org/10.4102/jamba.v2i1.15>
23. Calcaterra S, Cesi C, Di Maio C, Gambino P, Merli K, Vallari M, Vassallo R (2012) Surface displacements of two landslides evaluated by GPS and inclinometer systems: A case study in Southern Apennines, Italy. *Natural Hazards*61(1): 257–266. <https://doi.org/10.1007/s11069-010-9633-3>
24. Che V B, Kervyn M, Ernst G G J, Trefois P, Ayonghe S, Jacobs P, van Ranst E, Suh C E (2011). Systematic documentation of landslide events in Limbe area (Mt Cameroon Volcano, SW Cameroon): Geometry, controlling, and triggering factors. *Natural Hazards*59(1): 47–74. <https://doi.org/10.1007/s11069-011-9738-3>
25. Che V B, Kervyn M, Suh C E, Fontijn K, Ernst G G J, Del Marmol M A, Trefois P, Jacobs P (2012) Landslide susceptibility assessment in Limbe (SW Cameroon): A field calibrated seed cell and information value method. *Catena*92: 83–98. <https://doi.org/10.1016/j.catena.2011.11.014>

26. Chen CY, Huang W L (2013) Land use change and landslide characteristics analysis for community-based disaster mitigation. *Environmental Monitoring and Assessment*, 185(5): 4125–4139.
<https://doi.org/10.1007/s10661-012-2855-y>
27. Chen X L, Zhou Q, Ran H, Dong R (2012) Earthquake-triggered landslides in southwest China. *Natural Hazards and Earth System Sciences*12(2): 351–363. <https://doi.org/10.5194/nhess-12-351-2012>
28. Cina A, Piras M (2015) Performance of low-cost GNSS receiver for landslides monitoring: test and results. *Geomatics, Natural Hazards and Risk*6 (5–7): 497–514.
<https://doi.org/10.1080/19475705.2014.889046>
29. Ciurleo M, Cascini L, Calvello M (2017) A comparison of statistical and deterministic methods for shallow landslide susceptibility zoning in clayey soils. *Engineering Geology*223: 71–81.
<https://doi.org/10.1016/j.enggeo.2017.04.023>
30. Coe J A, Ellis W L, Godt, J W, Savage W Z, Savage J E, Michael J A, Kibler J D, Powers P S, Lidke J, Debray S (2003) Seasonal movement of the Slumgullion landslide determined from global positioning system surveys and field instrumentation, July 1998–March 2002. *Engineering Geology*68(1–2): 67–101. [https://doi.org/10.1016/S0013-7952\(02\)00199-0](https://doi.org/10.1016/S0013-7952(02)00199-0)
31. Couture R (2011) Landslide Terminology - National Technical Guidelines and Best Practices on Landslides. Geological Survey of Canada, Open File 6824.
32. Crozier M J (1986) Landslides: Causes, Consequences and Environment, Croom Helm, London, xvi + 252 p., 75 fig., 36 tabl., 14 x 22 cm, 25£. *Géographie Physique et Quaternaire*41(3): 409.
<https://doi.org/10.7202/032702ar>
33. Dai F C, Lee C F (2002) Landslide characteristics and slope instability modeling using GIS, Lantau Island, Hong Kong. *Geomorphology*, 42(3–4): 213–228. [https://doi.org/10.1016/S0169-555X\(01\)00087-3](https://doi.org/10.1016/S0169-555X(01)00087-3)
34. Dai F C, Lee C F, Li J, Xu Z W (2001) Assessment of landslide susceptibility on the natural terrain of Lantau Island, Hong Kong. *Environmental Geology*40(3): 381–391.
<https://doi.org/10.1007/s002540000163>
35. De Brito M M, Weber E J, Da Silva Filho L C P (2017) Multi-criteria analysis applied to landslide susceptibility mapping. *Revista Brasileira de Geomorfologia*18(4): 719–735.
<https://doi.org/10.20502/rbg.v18i4.1117>
36. Dhakal A S, Amada T, Aniya M (2000) Landslide hazard mapping and its evaluation using GIS: An investigation of sampling schemes for a grid-cell based quantitative method. *Photogrammetric Engineering and Remote Sensing*66(8): 981–989.
37. Diko M L (2012) Community engagement in landslide risk assessment in Limbe, Southwest Cameroon. *Scientific Research and Essays*7(32): 2906–2912. <https://doi.org/10.5897/sre12.488>
38. Diko M L (2012) Physical and geotechnical characterization of unconsolidated sediments associated with the 2005 Mbonjo landslide, Limbe, Cameroon. *International Journal of the Physical Sciences*7(20): <https://doi.org/10.5897/ijps12.066>

39. Donati L, Turrini M C (2002) An objective method to rank the importance of the factors predisposing to landslides with the GIS methodology: Application to an area of the Apennines (Valnerina; Perugia, Italy). *Engineering Geology*63(3–4): 277–289. [https://doi.org/10.1016/S0013-7952\(01\)00087-4](https://doi.org/10.1016/S0013-7952(01)00087-4)
40. Duman T Y, Can T, Gokceoglu C, Nefeslioglu H A (2005) Landslide susceptibility mapping of Cekmece area (Istanbul, Turkey) by conditional probability. *Hydrology and Earth System Sciences Discussions*2(1): 155–208. <https://doi.org/10.5194/hessd-2-155-2005>
41. Eastman J R, Jiang H (1995) Fuzzy measures in multi-criteria evaluation. In Proceedings, Second International Symposium on Spatial Accuracy Assessment in Natural Resources and Environmental Studies 21–23 (Fort Collins, Colorado)
42. Eastman J R (2012) The IDRISI Selva Help. Clark Labs, Clark University 950 Main Street, Worcester MA 01610–1477 USA
43. EM-DAT (2019) Disaster Year in Review 2019. *Cred*, 58, 1–2. Retrieved from <https://emdat.be/cred-crunch-58-disaster-year-review-2019> on 28 August 2020
44. Erener A, Mutlu A, Sebnem Düzgün H (2016) A comparative study for landslide susceptibility mapping using GIS-based multi-criteria decision analysis (MCDA), logistic regression (LR) and association rule mining (ARM). *Engineering Geology*203: 45–55. <https://doi.org/10.1016/j.enggeo.2015.09.007>
45. Feizizadeh B, Blaschke T (2013) GIS-multicriteria decision analysis for landslide susceptibility mapping: Comparing three methods for the Urmia lake basin, Iran. *Natural Hazards*65(3): 2105–2128. <https://doi.org/10.1007/s11069-012-0463-3>
46. Feizizadeh B, Shadman Roodposhti M, Jankowski P, Blaschke T (2014) A GIS-based extended fuzzy multi-criteria evaluation for landslide susceptibility mapping. *Computers and Geosciences*73: 208–221. <https://doi.org/10.1016/j.cageo.2014.08.001>
47. Fernandez T, Jimenez J, Delgado J, Cardenal J, Perez JL, Hamdouni R, Irigaray C, Chacon J (2013) Methodology for landslide susceptibility and Hazard mapping using GIS and SDI. Intelligent systems for crisis management, lecture notes in Geoinformation and Cartography 185–198. [http:// DOI: 10.1007/978-3-642-33218-0_14](http://DOI:10.1007/978-3-642-33218-0_14)
48. Francioni M, Calamita F, Coggan J, De Nardis A, Eyre M, Miccadei E, Piacentini T, Stead D, & Sciarra N (2019) A multi-disciplinary approach to the study of large rock avalanches combining remote sensing, GIS and field surveys: The case of the Scanno landslide, Italy. *Remote Sensing*11(13): <https://doi.org/10.3390/rs11131570>
49. Ge Y, Chen H, Zhao B, Tang H, Lin Z, Xie Z, Lv L, Zhong P (2018) A comparison of five methods in landslide susceptibility assessment: a case study from the 330-kV transmission line in Gansu Region, China. *Environmental Earth Sciences*77(19): 1–15. <https://doi.org/10.1007/s12665-018-7814-7>
50. Gigović L, Drobnjak S, Pamučar D (2019) The application of the hybrid GIS spatial multi-criteria decision analysis best–worst methodology for landslide susceptibility mapping. *ISPRS International Journal of Geo-Information*8(2): 1–29. <https://doi.org/10.3390/ijgi8020079>

53. Gili J A, Corominas J, Rius J (2000) Using Global Positioning System techniques in landslide monitoring. *Engineering Geology*55(3): 167–192. [https://doi.org/10.1016/S0013-7952\(99\)00127-1](https://doi.org/10.1016/S0013-7952(99)00127-1)
54. Gorsevski P V, Foltz R B (2000) Spatial Prediction of Landslide Hazard Using Discriminant Analysis and GIS GIS in the Rockies 2000 Conference. *Analysis, January 2000*.
55. Guedjeo C S, Dongmo K (2013) Natural hazards along the Bamenda escarpment and its environs: The case of landslide , rock fall and flood risks (Cameroon volcanic line , North-West Region). *Global Advanced Research Journal of Geology and Mining Research*2(1): 15–26.
56. Guillard C, Zezere J (2012) Landslide susceptibility assessment and validation in the framework of municipal planning in Portugal: The case of loures municipality. *Environmental Management*50(4): 721–735. <https://doi.org/10.1007/s00267-012-9921-7>
57. Guzzetti F, Carrara A, Cardinali M, Reichenbach P (1999) Landslide hazard evaluation: A review of current techniques and their application in a multi-scale study, Central Italy. *Geomorphology*31(1–4): 181–216. [https://doi.org/10.1016/S0169-555X\(99\)00078-1](https://doi.org/10.1016/S0169-555X(99)00078-1)
58. Holec J, Bednarik M, Šabo, M, Minár J, Yilmaz I, Marschalko M (2013) A small-scale landslide susceptibility assessment for the territory of Western Carpathians. *Natural Hazards*69(1): 1081–1107. <https://doi.org/10.1007/s11069-013-0751-6>
59. Huang F, Cao Z, Guo J, Jiang S H, Li S, Guo Z (2020) Comparisons of heuristic, general statistical and machine learning models for landslide susceptibility prediction and mapping. *Catena*191: 104580. <https://doi.org/10.1016/j.catena.2020.104580>
60. Jazouli A, Barakat A, Khellouk R (2019) GIS-multicriteria evaluation using AHP for landslide susceptibility mapping in Oum Er Rbia high basin (Morocco). *Geoenvironmental Disasters*6(1): <https://doi.org/10.1186/s40677-019-0119-7>
61. Ji S, Yu D, Shen C, Li ., Xu Q (2020) Landslide detection from an open satellite imagery and digital elevation model dataset using attention boosted convolutional neural networks. *Landslides*17(6): 1337–1352. <https://doi.org/10.1007/s10346-020-01353-2>
62. Jiang H, Eastman J R (2000) Application of Fuzzy Measures in MultiCriteria Evaluation in GIS. *International Journal of Geographical Information Science*14(2): 173–184.
63. Kavzoglu T, Sahin E K, Colkesen I (2014) Landslide susceptibility mapping using GIS-based multi-criteria decision analysis, support vector machines, and logistic regression. *Landslides*11(3): 425–439. <https://doi.org/10.1007/s10346-013-0391-7>
64. Keefer D K (2002) Investigating landslides caused by earthquakes - A historical review. *Surveys in Geophysics*23(6): 473–510. <https://doi.org/10.1023/A:1021274710840>
65. Kganyago M, Mhangara P (2019) The role of African emerging space agencies in earth observation capacity building for facilitating the implementation and monitoring of the African development agenda: The case of African earth observation program. *ISPRS International Journal of Geo-Information*8(7): <https://doi.org/10.3390/ijgi8070292>
66. Kirschbaum D B, Adler R, Hong Y, Hill S, Lerner-Lam A (2010) A global landslide catalog for hazard applications: Method, results, and limitations. *Natural Hazards*52(3): 561–575.

<https://doi.org/10.1007/s11069-009-9401-4>

67. Kometa S S (2012) Ensuring Human Safety in the Disaster Prone Coastal Town of Limbe, Cameroon. *Journal of Geography and Geology*4(2): 156–165. <https://doi.org/10.5539/jgg.v4n2p156>
68. Kouankap Nono G D, Nzenti J P, Suh C E, Ganno S (2010) Geochemistry of Ferriferous, High-K Calc-Alkaline Granitoids from the Banefo-Mvoutsaha Massif (NE Bafoussam), Central Domain of the Pan-African Fold Belt, Cameroon~!2009-11-12~!2010-01-05~!2010-03-11~! *The Open Geology Journal*4(1): 15–28. <https://doi.org/10.2174/1874262901004010015>
69. Kouankap Nono G D , Wotchoko P, Ganno S, Njinchuki N, Nzenti J P (2013) Petrochemical Characterization of Two Distinct Types of Dolerites from Bafoussam Area, West Cameroon. *International Journal of Geosciences*04(08): 1131–1144. <https://doi.org/10.4236/ijg.2013.48107>
70. Kritikos T, Davies T R H (2011) GIS-basierte multikriterielle entscheidungsanalysen zur kartierung von massenverlagerungspotenzialen im nördlichen Evia, Griechenland. *Zeitschrift Der Deutschen Gesellschaft Fur Geowissenschaften*162(4): 421–434. <https://doi.org/10.1127/1860-1804/2011/0162-0421>
71. Kumar M (2005) Digital Image Processing. Satellite Remote Sensing and GIS applications in Agricultural meteorology. pp. 81-102
72. Kumar A, Sharma R K, Bansal V K (2018) Landslide hazard zonation using analytical hierarchy process along National Highway-3 in mid Himalayas of Himachal Pradesh, India. *Environmental Earth Sciences*77(20): 1–19. <https://doi.org/10.1007/s12665-018-7896-2>
73. Kumar R, Anbalagan R (2016) Landslide susceptibility mapping using analytical hierarchy process (AHP) in Tehri reservoir rim region, Uttarakhand. *Journal of the Geological Society of India*87(3): 271–286. <https://doi.org/10.1007/s12594-016-0395-8>
74. Leoni G, Campolo D, Falconi L, Gioe C, Lumaca S, Puglisi C, Torre A (2015) Heuristic Method for Landslide Susceptibility Assessment in the Messina Municipality. *Engineering Geology for Society and Territory* 2: 501-504. [https:// DOI: 10.1007/978-3-319-09057-3_82](https://doi.org/10.1007/978-3-319-09057-3_82)
75. Liu Y, Wu L (2016) Geological Disaster Recognition on Optical Remote Sensing Images Using Deep Learning. *Procedia Computer Science*91: 566–575. <https://doi.org/10.1016/j.procs.2016.07.144>
76. Lu D, Weng Q (2007) A survey of image classification methods and techniques for improving classification performance. *International Journal of Remote Sensing*28(5): 823–870. <https://doi.org/10.1080/01431160600746456>
77. Ly S, Charles C, Degré (2013) Different methods for spatial interpolation of rainfall data for operational hydrology and hydrological modeling at watershed scale. A review. *Biotechnol. Agron. Soc. Environ* 17(2): 392-406
78. Malczewski J (2004) GIS-based land-use suitability analysis: A critical overview. *Progress in Planning*62(1): 3–65. <https://doi.org/10.1016/j.progress.2003.09.002>
79. Malet J P, Maquaire O, Calais E (2002) The use of global positioning system techniques for the continuous monitoring of landslides: Application to the Super-Sauze earthflow (Alpes-de-Haute-

- Provence, France). *Geomorphology*43(1–2): 33–54. [https://doi.org/10.1016/S0169-555X\(01\)00098-8](https://doi.org/10.1016/S0169-555X(01)00098-8)
80. Manzo G, Tofani V, Segoni S, Battistini A, Catani F (2013) GIS techniques for regional-scale landslide susceptibility assessment: The Sicily (Italy) case study. *International Journal of Geographical Information Science*27(7): 1433–1452. <https://doi.org/10.1080/13658816.2012.693614>
 81. Marzoli A, Piccirillo E M, Renne P R, Bellieni G, Iacumin M, Nyobe J B, Tongwa A T (2000). The cameroon volcanic line revisited: Petrogenesis of continental basaltic magmas from lithospheric and asthenospheric mantle sources. *Journal of Petrology*41(1): 87–109. <https://doi.org/10.1093/petrology/41.1.87>
 82. Matossian A O, Baghdasaryan H, Avagyan A, Igityan H, Gevorgyan M. Havenith H B (2020) A new landslide inventory for the armenian lesser caucasus: Slope failure morphologies and seismotectonic influences on large landslides. *Geosciences* 10(3): <https://doi.org/10.3390/geosciences10030111>
 83. Mergili M, Schwarz L, Kociu A (2019) Combining release and runout in statistical landslide susceptibility modeling. *Landslides*16(11): 2151–2165. <https://doi.org/10.1007/s10346-019-01222-7>
 84. Moeyersons J, Van Den Eeckhaut M, Nyssen J, Gebreyohannes T, Van de Wauw J, Hofmeister J, Poesen J, Deckers J, Mitiku H (2008) Mass movement mapping for geomorphological understanding and sustainable development: Tigray, Ethiopia. *Catena*75(1): 45–54. <https://doi.org/10.1016/j.catena.2008.04.004>
 85. Nandi A, Shakoor A (2010) A GIS-based landslide susceptibility evaluation using bivariate and multivariate statistical analyses. *Engineering Geology*110(1–2): 11–20. <https://doi.org/10.1016/j.enggeo.2009.10.001>
 86. Ngatcha B N, Ekodeck G E, Mpele M, Ntana P E (2011) Hydrological and geotechnical investigations of mass movements in an equatorial city (Yaoundé, Cameroon). *Environmental Earth Sciences*62(8): 1733–1747. <https://doi.org/10.1007/s12665-010-0654-8>
 87. Ngole V, Georges-Ivo E, Ayonghe S (2010) Physico-chemical, mineralogical and chemical considerations in understanding the 2001 Mabeta New Layout landslide, Cameroon. *Journal of Applied Sciences and Environmental Management*11(2): <https://doi.org/10.4314/jasem.v11i2.55041>
 88. Nichol J, Wong M S (2005) Detection and interpretation of landslides using satellite images. *Land Degradation and Development*16(3): 243–255. <https://doi.org/10.1002/ldr.648>
 89. Nicu I C (2018) Application of analytic hierarchy process, frequency ratio, and statistical index to landslide susceptibility: an approach to endangered cultural heritage. *Environmental Earth Sciences*77(3): 1–16. <https://doi.org/10.1007/s12665-018-7261-5>
 90. Ntasin E, Ayonghe S, Suh C (2009) Slope Stability Studies Of Wabane Caldera, Western Cameroon: Impact Of Hydrology, Hydrogeology And Human Factors On Landslide Initiation. *Global Journal of Pure and Applied Sciences*15(1): 79–90. <https://doi.org/10.4314/gjpas.v15i1.44900>

91. Ntchantcho R, Anye L N, Aka F T, Kankeu B, Buh G. W, Ndifon P T, Nnange J M, Hell J V (2017) The Debris Flow of 1st August 2012 in Kakpenyi-Tinta (Akwaya Sub Division) Southwest Cameroon—I: Event Description, Causes and Impacts. *Open Journal of Geology*07(09): 1337–1351. <https://doi.org/10.4236/ojg.2017.79089>
92. Nzotcha U, Kenfack J, Blanche Manjia M (2019) Integrated multi-criteria decision making methodology for pumped hydro-energy storage plant site selection from a sustainable development perspective with an application. *Renewable and Sustainable Energy Reviews*112): 930–947. <https://doi.org/10.1016/j.rser.2019.06.035>
93. Osanai N, Yamada T, Hayashi S, Ichiro, Kastura S, Furuichi T, Yanai S, Murakami Y, Miyazaki T, Tanioka Y, Takiguchi S, Miyazaki M (2019) Characteristics of landslides caused by the 2018 Hokkaido Eastern Iburi Earthquake. *Landslides*16(8): 1517–1528. <https://doi.org/10.1007/s10346-019-01206-7>
94. Pardeshi S D, Autade S E, Pardeshi S S (2013) Landslide hazard assessment: Recent trends and techniques. *SpringerPlus*2(1): 1–11. <https://doi.org/10.1186/2193-1801-2-523>
95. Park S, Choi C, Kim B, Kim J (2013) Landslide susceptibility mapping using frequency ratio, analytic hierarchy process, logistic regression, and artificial neural network methods at the Inje area, Korea. *Environmental Earth Sciences*68(5): 1443–1464. <https://doi.org/10.1007/s12665-012-1842-5>
96. Pearson A W (2006) Digitizing and analysing historical maps to provide new perspectives on the development of the agricultural landscape of England and Wales. *E-Perimtron*1(3): 178–193.
97. Petley D N, Crick W D O, Hart A B (2002) The use of satellite imagery in landslide studies in high mountain areas. *Proceedings of the 23th Asian Conference on Remote Sensing, Kathmandu*.
98. Pradhan B (2013) A comparative study on the predictive ability of the decision tree, support vector machine and neuro-fuzzy models in landslide susceptibility mapping using GIS. *Computers and Geosciences*51: 350–365. <https://doi.org/10.1016/j.cageo.2012.08.023>
99. Rajakumar P, Sanjeevi S, Jayaseelan S, Isakkipandian G, Edwin M, Balaji P, Ehanthalingam G (2007) Landslide susceptibility mapping in a hilly terrain using remote sensing and GIS. *Journal of the Indian Society of Remote Sensing*35(1): 31–42. <https://doi.org/10.1007/BF02991831>
100. Regmi N R, Giardino J R, Vitek J D (2010) Modeling susceptibility to landslides using the weight of evidence approach: Western Colorado, USA. *Geomorphology*115(1–2): 172–187. <https://doi.org/10.1016/j.geomorph.2009.10.002>
101. Reichenbach P, Busca C, Mondini A C, Rossi M (2014) The Influence of Land Use Change on Landslide Susceptibility Zonation: The Briga Catchment Test Site (Messina, Italy). *Environmental Management*54(6): 1372–1384. <https://doi.org/10.1007/s00267-014-0357-0>
102. Reichenbach P, Rossi M, Malamud B D, Mihir M, Guzzetti F (2018) A review of statistically-based landslide susceptibility models. *Earth-Science Reviews* 180: 60–91
103. Ruff M, Czurda K (2008) Landslide susceptibility analysis with a heuristic approach in the Eastern Alps (Vorarlberg, Austria). *Geomorphology*94(3–4): 314–324. <https://doi.org/10.1016/j.geomorph.2006.10.032>

104. Saaty T L (2008) Decision Making with the Analytical Hierarchy Process. *Int. J. Services Sciences* 1 (1): 83-98
105. Saaty R W (1987) The analytic hierarchy process-what it is and how it is used. *Mathematical Modelling* (3–5): 161–176. [https://doi.org/10.1016/0270-0255\(87\)90473-8](https://doi.org/10.1016/0270-0255(87)90473-8)
106. Saaty T L (1986) Absolute and relative measurement with the AHP. The most livable cities in the United States. *Socio-Economic Planning Sciences* 20(6): 327–331. [https://doi.org/10.1016/0038-0121\(86\)90043-1](https://doi.org/10.1016/0038-0121(86)90043-1)
107. Saaty TL (1977) A scaling method for priorities in hierarchical structures. *J Math Psychol* 15: 231–281 [https://doi.org/10.1016/0022-2496\(77\)90033-5](https://doi.org/10.1016/0022-2496(77)90033-5)
108. Santacana N, Baeza B, Corominas J De Paz A (2003) A GIS multicriteria statistical analysis for shallow landslide susceptibility mapping in La Pobla de Lillet area eastern Pyrenees, Spain. *Natural Hazards* 30: 281-295
109. Sartohadi J, Pulungan N A . Jennie, Nurudin M Wahyudi W (2018) The Ecological Perspective of Landslides at Soils with High Clay Content in the Middle Bogowonto Watershed, Central Java, Indonesia. *Applied and Environmental Soil Science* 1-9: <https://doi.org/10.1155/2018/2648185>
110. Schilirò L, Poueme Djueyep G, Esposito C, Scarascia Mugnozza, G (2019) The Role of Initial Soil Conditions in Shallow Landslide Triggering: Insights from Physically Based Approaches. *Geofluids* 1-14. <https://doi.org/10.1155/2019/2453786>
111. Shahabi H Ahmad B B, Khezri S (2012) Landslide Susceptibility Mapping Using Image Satellite and GIS Technology Department of Remote sensing, Faculty of Geo Information and Real Estate , universiti Teknologi. *International Journal of Engineering Research & Technology* 1(6): 2–6.
112. Shahabi H, Hashim M (2015) Landslide susceptibility mapping using GIS-based statistical models and Remote sensing data in tropical environment. *Scientific Reports* 5: 1–15. <https://doi.org/10.1038/srep09899>
113. Shi X, Zhang L, Zhong Y, Zhang L, Liao M (2020) Detection and characterization of active slope deformations with Sentinel-1 InSAR analyses in the southwest area of Shanxi, China. *Remote Sensing* 12(3): <https://doi.org/10.3390/rs12030392>
114. Stanley T, Kirschbaum D B (2017) A heuristic approach to global landslide susceptibility mapping. *Natural Hazards* 87(1): 145–164. <https://doi.org/10.1007/s11069-017-2757-y>
115. Suh C E, Sparks R S J, Fitton J G, Ayonghe S N, Annen C, Nana R, Luckman A (2003) The 1999 and 2000 eruptions of Mount Cameroon: Eruption behaviour and petrochemistry of lava. *Bulletin of Volcanology* 65(4): 267–281. <https://doi.org/10.1007/s00445-002-0257-7>
116. Tesi, M.K (2018). Cameroon Western Region: Environmental disaster in the making? In: Abbink (ed) The environmental crunch in Africa, Springer International, 179-205 https://doi.org/10.1007/978-3-319-77131-1_7
117. Thierry P, Stieltjes L, Kouokam E, Nguéya P, Salley P M (2008) Multi-hazard risk mapping and assessment on an active volcano: The GRINP project at Mount Cameroon. *Natural Hazards* 45(3): 429–456. <https://doi.org/10.1007/s11069-007-9177-3>

118. Toteu S F, Van Schmus W R, Penaye J, Michard A (2001) New U-Pb and Sm-Nd data from north-central Cameroon and its bearing on the pre-Pan African history of Central Africa. *Precambrian Research*108(1–2): 45–73. [https://doi.org/10.1016/S0301-9268\(00\)00149-2](https://doi.org/10.1016/S0301-9268(00)00149-2)
119. Van Den Eeckhaut M, Vanwallegghem T, Poesen J, Govers G, Verstraeten G, Vandekerckhove L (2006) Prediction of landslide susceptibility using rare events logistic regression: A case-study in the Flemish Ardennes (Belgium). *Geomorphology*76(3–4): 392–410. <https://doi.org/10.1016/j.geomorph.2005.12.003>
120. Van Schmus W R, Oliveira E P, Da Silva Filho A F, Toteu S F, Penay, J, Guimarães I P.(2008). Proterozoic links between the Borborema Province, NE Brazil, and the Central African fold belt. *Geological Society Special Publication*294: 69–99. <https://doi.org/10.1144/SP294.5>
121. Van Westen C. (2000) Remote sensing for natural disaster management. *International Archives of the Photogrammetry, Remote Sensing and Spatial Information Sciences - ISPRS Archives*33(January 2000).
122. Van Westen C J, Rengers N, Soeters R (2003) Use of Geomorphological expert knowledge in indirect landslide hazard assessment. *Natural Hazards*30: 399–419.
123. van Westen C J, Castellanos E, Kuriakose S L (2008) Spatial data for landslide susceptibility, hazard, and vulnerability assessment: An overview. *Engineering Geology*102(3–4):112–131. <https://doi.org/10.1016/j.enggeo.2008.03.010>
124. VanBuskirk C D, Neden R.J, Schwab JW Smith F R (BC Ministry of Forests and Range, R. B. (2005). *Road and Terrain Attributes of Road Fill Landslides in the Kalum Forest District - BC Technical Report 024*. 61.
125. Vargas L G Zoffer H J (2019) Applying Analytical Hierarchy Process in conflict resolution. *International Journal of the Analytical Hierarchy Process* 11 (1): 1-20
126. Varnes D J (1984) Landslide Hazard Zonation: A Review of Principles and Practice, Natural Hazards UNESCO, Paris.
127. Vojteková J, Vojtek M (2020) Assessment of landslide susceptibility at a local spatial scale applying the multi-criteria analysis and GIS: a case study from Slovakia. *Geomatics, Natural Hazards and Risk*11(1): 131–148. <https://doi.org/10.1080/19475705.2020.1713233>
128. Wang B, Ruel M, Couture R, Bobrowsky P T, Blais-Stevens A (2012) *Review of existing landslide guidelines-National technical guidelines and best practices on landslides*. January, 13. <https://doi.org/10.4095/289864>
129. Wantim M N, Kervyn M, Ernst G. G J, Marmol M-A Del, Suh C E, Jacobs P (2013) Morpho-Structure of the 1982 Lava Flow Field at Mount Cameroon Volcano, West-Central Africa. *International Journal of Geosciences*04(03): 564–583. <https://doi.org/10.4236/ijg.2013.43052>
130. Wotchoko P, Bardintzeff J M , Itiga Z, Nkouathio D G, Guedjeo C S, Ngnoupeck G, Dongmo A K, Wandji P (2016) Geohazards (floods and landslides) in the Ndop plain Cameroon volcanic line. *Open Geosciences*8(1): 429–449. <https://doi.org/10.1515/geo-2016-0030>

131. Xu C, Xu X, Lee Y H, Tan X, Yu G, Dai F (2012) The 2010 Yushu earthquake triggered landslide hazard mapping using GIS and weight of evidence modeling. *Environmental Earth Sciences*66(6): 1603–1616. <https://doi.org/10.1007/s12665-012-1624-0>
132. Yalcin A, Reis S, Aydinoglu A C, Yomralioglu T (2011) A GIS-based comparative study of frequency ratio, analytical hierarchy process, bivariate statistics and logistics regression methods for landslide susceptibility mapping in Trabzon, NE Turkey. *Catena*85(3): 274–287. <https://doi.org/10.1016/j.catena.2011.01.014>
133. Yin Y, Wang F, Sun P (2009) Landslide hazards triggered by the 2008 Wenchuan earthquake, Sichuan, China. *Landslides*6(2): 139–152. <https://doi.org/10.1007/s10346-009-0148-5>
134. Zaitunah A, Samsuri, Ahmad A G, Safitri R A (2018) Normalized difference vegetation index (NDVI) analysis for landcover types using landsat 8 OLI in Besitang watershed, Indonesia. IOP Conf. Series: Earth and Environmental Science 126: 012112. <https://doi.org/10.1088/1755-1315/126/1/012112>
135. Zangmo G T, Kagou A D, Nkouathio G Wandji P (2009) Typology of natural hazards and Assessment of associated risks in the Mount Bamboutos Caldera (Cameroon Line, West Cameroon). *Acta Geologica Sinica* 83: 1008-1016.
136. Zêzere J L, Pereira S, Melo R, Oliveira S C, Garcia R A C (2017) Mapping landslide susceptibility using data-driven methods. *Science of the Total Environment*589: 250–267. <https://doi.org/10.1016/j.scitotenv.2017.02.188>
137. Zhao B, Wang Y S, Luo Y H Li J, Zhang X, Shen T (2018) Landslides and dam damage resulting from the jiuzhaigou earthquake (8 august 2017), Sichuan, China. *Royal Society Open Science*5(3). <https://doi.org/10.1098/rsos.171418>
138. Zhong C, Liu,Y, Gao P, Chen W, Li H, Hou Y, NuremanguliT Ma H (2020) Landslide mapping with remote sensing: challenges and opportunities. *International Journal of Remote Sensing*41(4) 1555–1581. <https://doi.org/10.1080/01431161.2019.1672904>
139. Zogning A, Ngouanet C, Tiafack O (2007) The catastrophic geomorphological processes in humid tropical Africa: A case study of the recent landslide disasters in Cameroon. *Sedimentary Geology*199(1–2): 13–27. <https://doi.org/10.1016/j.sedgeo.2006.03.030>

9. Tables

Table 1
Input data set, format, generated layers and data source used in the study

Input data	Format	Map layer generated	Data source
SRTM DEM (30 m)	Raster	Aspect	USGS website (https://earthexplorer.usgs.gov/)
		Slope	
		Elevation	
Landsat 8 OLI Image (30 m)	Raster	Landuse map	USGS website (https://earthexplorer.usgs.gov/)
		NDVI	
Geology (1: 1, 000, 000 scale)	Raster	Lithology map	Van Schmus et al. 2008
	Shapefile	Distance to fault	
Soils	Shapefile	Soil map	Africa Groundwater Atlas, 2019
Rainfall	Raster	Average monthly rainfall	NASA Earth Science Data (https://giovanni.gsfc.nasa.gov/)
Roads	Shapefile	Distance to road	OpenStreet Map (openstreetmap.org)
Rivers	Shapefile	Distance to river	

Table 2
Proposed scale for factor weighting in MCDA (adopted from Saaty 1987)

Intensity of Importance	The verbal judgement of preference
Equal Importance	
3	Moderate importance
5	Strong importance
7	Very strong importance
9	Extreme importance
2,4,6,8	Intermediate values between adjacent scale values

Table 3

Random consistency index for deriving consistency ratio (Adopted from Saaty 1987)

Factors (n)	1	2	3	4	5	6	7	8	9	10
Random index (RI)	0	0	0.58	0.90	1.12	1.24	1.32	1.41	1.45	1.49

Table 4

Landslide inventory derived from review of literature and satellite image analysis

Location of slide	Date	Source	Casualties/Damage
Bamboutos	July 2003	Ayonghe and Ntasin, 2008	23 deaths, 700 livestock killed, 1000 persons displaced
Bamboutos	July 2003	Ayonghe and Ntasin, 2008	
Bamboutos	July 2003	Ayonghe and Ntasin, 2008	
Bamboutos	July 2003	Ayonghe and Ntasin, 2008	
Bakombo	June 1988	Ayonghe et al. 1999	8 deaths, property damage
Foungwo			
Gouata	September 1997	Ayonghe et al. 1999	1 dead, damage to farmland
Echiok	Unknown	Deduced from satellite images	Unknown
Bapi	Unknown	Deduced from satellite images	Unknown
Ngwenfon	Unknown	Deduced from satellite images	Unknown
Ngwenfon	Unknown	Deduced from satellite images	Unknown
Ngwenfon	Unknown	Deduced from satellite images	Unknown
Bassinte	Unknown	Deduced from satellite images	Unknown
Makpa	Unknown	Deduced from satellite images	Unknown
Gouache	October 2019	Cameroon News Agency	42 Deaths

Table 5
Pairwise comparison matrix, consistency index (CI), consistency ratio (CR) and weights of sub-factors

Slope	a	b	c	d	e	Weights
(a) 0-15.4	1					0.03
(b) 15.41–30.8	3.00	1				0.07
(c) 30.81–46.2	5	2	1			0.13
(d) 46.21–61.6	7	5	4	1		0.31
(e) 61.61–77	9	8	3	2	1	0.45
CI	0.044					
CR	0.039					
Geology	a	b	c	d		
(a) Pre-Syn Granitoid	1					0.05
(b) Syn-Post Granitoid	3	1				0.12
(c) Orthogneiss	5	3	1			0.24
(d) Volcanics	7	5	4	1		0.59
CI	0.058					
CR	0.07					
Soils	a	b	c	d	e	
(a) Andosols	1					0.23
(b) Loxisols	0.2	1				0.08
(c) Luvisols	2	3	1			0.20
(d) Stagnosols	0.17	0.33	0.5	1		0.05
(e) Vertisols	2	5	3	7	1	0.44
CI	0.111					
CR	0.09					
Elevation	a	b	c	d	e	
(a) 13–53	1					0.03
(b) 54–115	3	1				0.07

Slope	a	b	c	d	e	Weights
(c) 115–188	5	3	1			0.13
(d) 189–258	7	5	3	1		0.29
(e) 259–296	9	6	5	2	1	0.47
CI	0.048					
CR	0.042					
Fault	a	b	c	d	e	
(a) 5	1					0.47
(b) 10	0.33	1				0.29
(c) 15	0.2	0.33	1			0.13
(d) 20	0.14	0.2	0.33	1		0.07
(e) 25	0.11	0.17	0.2	0.5	1	0.03
CI	0.065					
CR	0.042					

Table 5
Continued

Aspect	a	b	c	d	e	f	g	h	weight
(a) North	1								0.03
(b) North East	2	1							0.05
(c) East	4	3	1						0.09
(d) South East	7	5	4	1					0.26
(e) South	7	5	4	1	1				0.26
(f) South West	5	3	2	0.5	0.5	1			0.15
(g) West	4	2	1	0.2	0.2	0.5	1		0.08
(h) North West	4	2	1	0.2	0.2	0.5	1	1	0.08
CI	0.076								
CR	0.052								
Land use	a	b	c	d	e				Weight
(a) Water Body	1								0.07
(b) Vegetation	3	1							0.16
(c) Built up Area	0.5	0.33	1						0.06
(d) Agricultural land	7	3	5	1					0.44
(e) Bare Soil	5	2	4	0.5	1				0.27
CI	0.036								
CR	0.032								
NDVI	a	b	c	d	e				
(a) 0.12 – 0.06	1								0.05
(b) 0.07-0.17	3	1							0.13
(c) 0.18–0.23	7	5	1						0.50
(d) 0.24–0.29	4	3	0.33	1					0.25
(e) 0.30–0.58	2	0.33	0.2	0.25	1				0.07
CI	0.057								
CR	0.051								

Aspect	a	b	c	d	e	f	g	h	weight
Distance from Rivers	a	b	c	d	e				
(a) 1	1								0.47
(b) 2	0.33	1							0.29
(c) 3	0.2	0.33	1						0.13
(d) 4	0.14	0.2	0.33	1					0.07
(e) 5	0.11	0.17	0.2	0.5	1				0.03
CI	0.048								
CR	0.042								
Distance from Roads	a	b	c	d	e				
(a) 1	1								0.47
(b) 2	0.33	1							0.29
(c) 3	0.2	0.33	1						0.13
(d) 4	0.14	0.2	0.33	1					0.07
(e) 5	0.11	0.17	0.2	0.5	1				0.03
CI	0.048								
CR	0.042								
Rainfall	a	b	c	d	e				
(a) 0.12–0.15	1								0.03
(b) 0.16-0.17	3	1							0.07
(c) 0.18–0.19	5	3	1						0.13
(d) 0.20–0.21	7	5	3	1					0.29
(e) 0.22–0.23	9	6	5	2	1				0.47
CI	0.048								
CR	0.042								

Table 6
Normalised pairwise comparison matrix, consistency ratio and factor weights

	a	b	c	d	e	f	g	h	i	j	k	Weight
(a) Slope	1	2	3	3	1	7	8	8	5	9	2	0.23
(b) Geology	0.5	1	2	2	0.33	5	7	7	4	7	1	0.14
(c) Soils	0.5	0.33	1	1	0.33	5	6	6	3	5	0.33	0.09
(d) Aspect	0.5	0.33	1	1	0.33	4	2	2	0.5	3	0.33	0.05
(e) Elevation	1	3	3	3	1	6	7	7	5	7	3	0.23
(f) Rainfall	0.14	0.2	0.2	0.25	0.17	1	2	2	0.33	3	0.2	0.03
(g) Road	0.13	0.14	0.17	0.5	0.14	0.5	1	1	0.33	2	0.14	0.02
(h) Rivers	0.13	0.14	0.17	0.5	0.14	0.2	1	1	0.33	2	0.14	0.02
(i) Landuse	0.2	0.25	0.33	2	0.2	3	3	3	1	4	0.25	0.05
(j) NDVI	0.11	0.14	0.2	0.33	0.14	0.33	0.5	0.5	0.25	1	0.14	0.01
(k) Fault	0.5	1	2	2	0.33	5	7	7	4	7	1	0.14
CI	0.07											
CR	0.04											

Table 7
Area, percentage coverage and validation of landslide classes

Landslide class	Area (km²)	Area (%)	% of inventory
Very Low	2051	15	0
Low	3149	23	21
Medium	6512	47	36
High	230	2	14
Very High	1950	14	29
Total	13892	100	

Figures

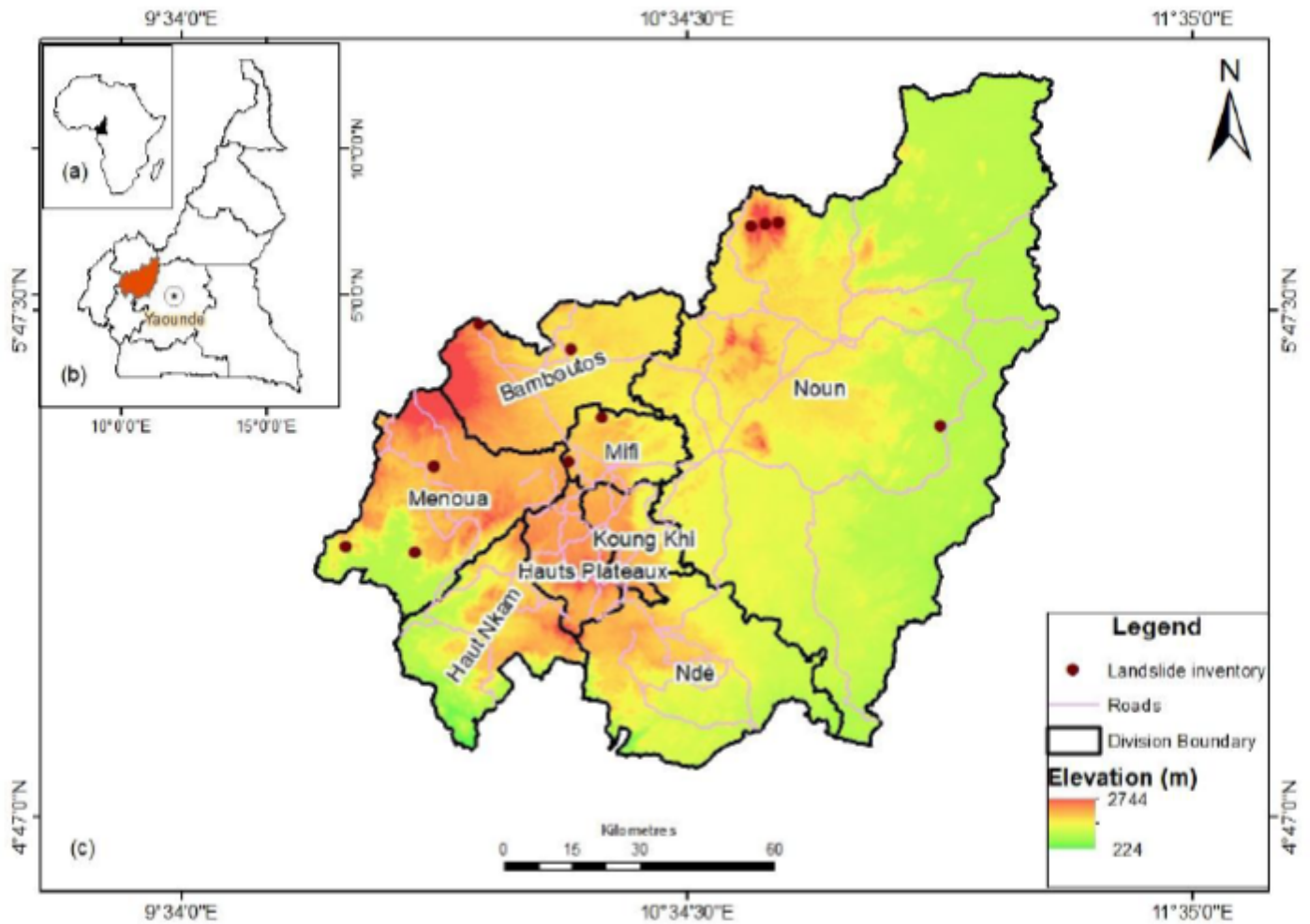


Figure 1

Location of study, (a) Inset of African map indicating the location of Cameroon (dark polygon). (b) Inset map of Cameroon showing the West Region (gold polygon). (c) Study area, the Divisions (Departments) in the West Region of Cameroon and landslide inventory

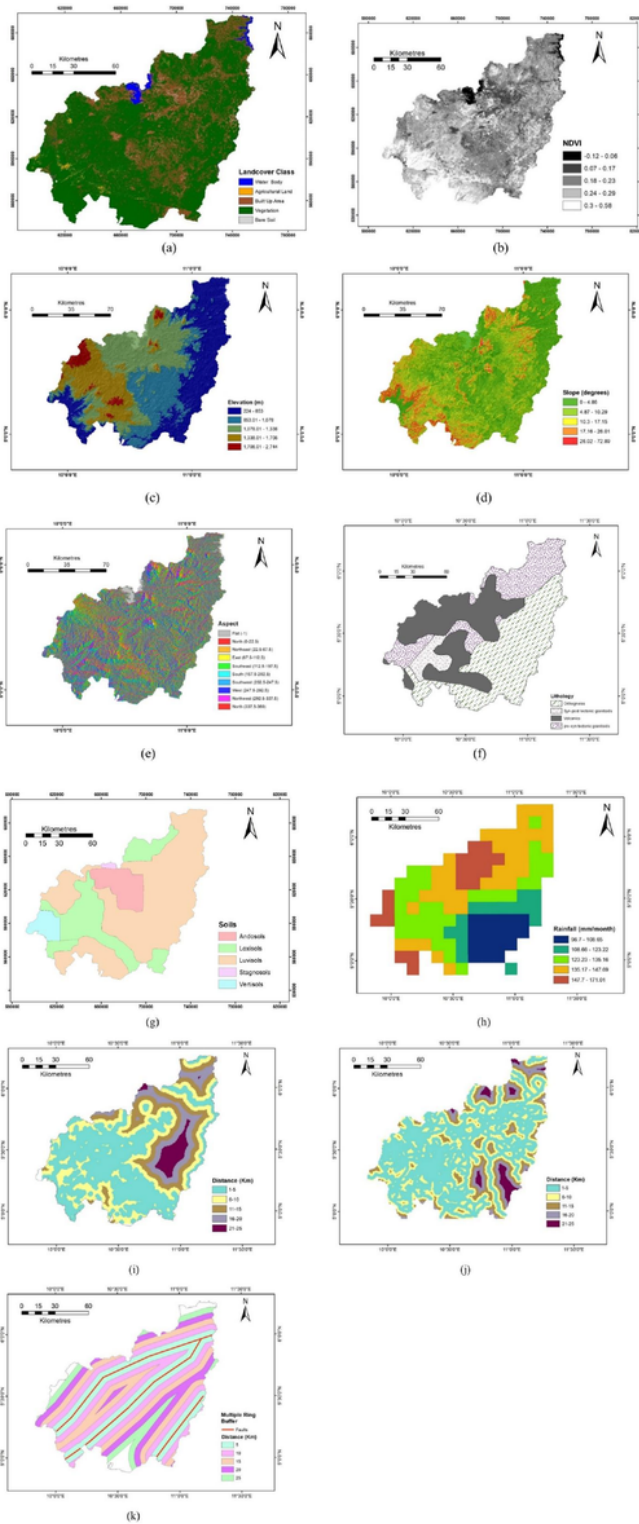


Figure 2

Thematic maps a) Landcover over 50% of the study area is covered with vegetation b) NDVI Normalized difference vegetation index map representing vegetation cover in the study area, light colour represent vegetation while dark colour indicates non-vegetated areas c) Elevation of the study area reclassified into five classes d) slope angle the slope ranges from 3o to 77o with an average of 40o e) Aspect f) Lithology of the study area, metamorphic and volcanic rocks make up a bulk of the lithology (adopted from Toteu

et al. 2001; Van Schmus et al. 2008) g) Soils h) Average monthly rainfall data (mm/month) from 2000-2020 i) Euclidean distance of roads j) Euclidean distance of rivers k) multiple ring buffer for distance to faults

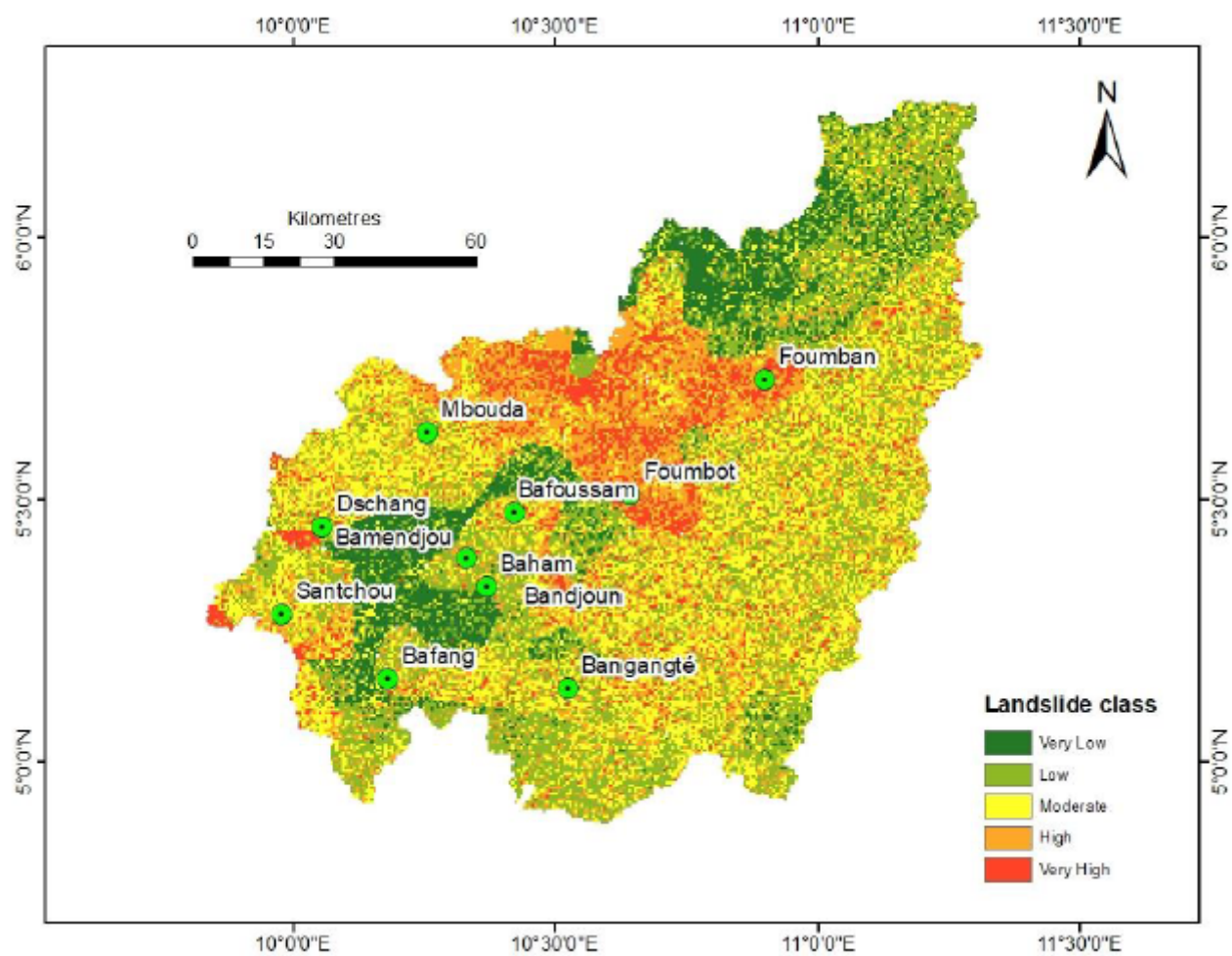


Figure 3

Landslide susceptibility map derived from the weighted linear combination of 11 conditioning factors

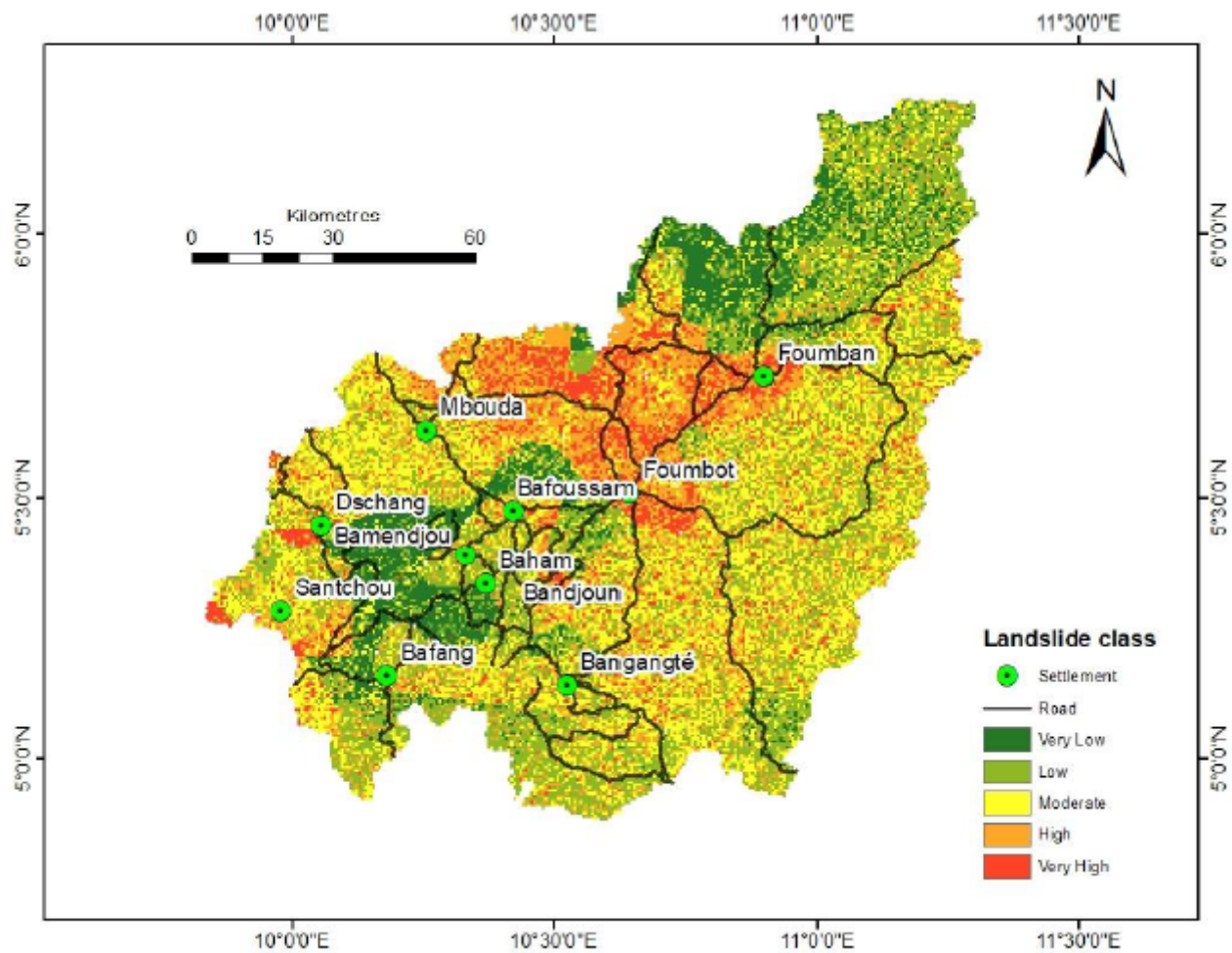


Figure 4

Roads and urban areas in high to very high landslide susceptibility zones

Supplementary Files

This is a list of supplementary files associated with this preprint. Click to download.

- [appendix.png](#)